Quiñones, DR.; Fernández-Mollá, LM.; Pacheco-Torres, J.; Caramés, JM.; Canals, S.; Moratal, D. (2019). TherMouseDuino: An affordable Open-Source temperature control system for functional magnetic resonance imaging experimentation with mice. Magnetic Resonance Imaging. 58:67-75. https://doi.org/10.1016/j.mri.2019.01.009

TherMouseDuino: An affordable Open-Source temperature control system for functional Magnetic Resonance Imaging experimentation with mice

Darío R. Quiñones[a], Luis Miguel Fernández-Mollá[a], Jesús Pacheco-Torres[b], José M. Caramés[b], Santiago Canals[b], David Moratal[a]

[a] *Centre for Biomaterials and Tissue Engineering, Universitat Politècnica de València, Camí de Vera s/n, 46022, Valencia, Spain*
[b] *Instituto de Neurociencias, Consejo Superior de Investigaciones Científicas – Universidad Miguel Hernández, Santiago Ramón y Cajal s/n, 03550 Sant Joan d'Alacant, Alicante, Spain.*

Abstract

Introduction: Functional magnetic resonance imaging (fMRI) is one of the most highly regarded techniques in the neuroimaging field. This technique is based on vascular responses to neuronal activation and is extensively used in clinical and animal research studies. In preclinical settings, fMRI is usually applied to anesthetized animals. However, anesthetics cause alterations, e.g. hypothermia, in the physiology of the animals and this has the potential to disrupt fMRI signals. The current temperature control method involves a technician, as well as monitoring the acquisition MRI sequences, also controlling the temperature of the animal; this is inefficient. *Methods:* In order to avoid hypothermia in anesthetized rodents an Open-Source automatic temperature control device is presented. It takes signals from an intrarectal temperature sensor, as well as signals from a thermal bath, which warms up the body of the animal under study, in order to determine the mathematical model of the thermal response of the animal. *Results:* A Proportional-Integral-Derivative (PID) algorithm, which was discretized in an Arduino microcontroller, was developed to automatically keep stable the body temperature of the animal under study. The

*David Moratal, PhD
Email address: dmoratal@eln.upv.es (David Moratal)

PID algorithm has been shown to be accurate in preserving the body temperature of the animal. *Conclusion:* This work presents the TherMouseDuino. It is an Open-Source automatic temperature control system and reduces temperature fluctuations, thus providing robust conditions in which to perform fMRI experiments. Furthermore, our device frees up the technician to focus solely on monitoring the MRI sequences.

Keywords: Anesthetic, Arduino, BOLD, fMRI, mice, PID

1. Introduction

Functional Magnetic Resonance Imaging (fMRI) is a non-invasive imaging technique that allows in vivo and longitudinal investigations of brain function. The Blood-Oxygen-Level Dependent (BOLD) signal is the most commonly used fMRI contrast to study brain activity [1, 2]. BOLD depends on a number of factors, including the different magnetic properties of oxygenated and deoxygenated hemoglobin, cerebral blood volume (CBV) and flow (CBF) [3, 4, 5].

Neuronal activity has an associated level of energy consumption [6, 7]. This energy is produced through chemical processes that require glucose and oxygen, the latter being transported in blood by the molecule hemoglobin. An increase in neuronal activity in an area of the brain immediately produces a higher ratio of oxygen extraction from the capillary network and therefore an increase in the concentration of deoxygenated hemoglobin. This initial blood deoxygenation is overcompensated by a vascular response increasing CBF and CBV around the activated brain area, a phenomenon known as neuro-vascular coupling and that represents the origin of the BOLD signal [1, 2]. Not surprisingly, the BOLD signal is influenced by a number of physiological parameters not directly related with neuronal signaling and cognitive processes, but directly coupled to vascular responses, such as temperature, blood pressure, CO_2 and O_2 concentration, pH and others. Nevertheless, a high correspondence between the BOLD signal and brain activity has been observed in well-controlled experiments [8, 9, 10, 11, 12, 13].

Currently, preclinical research is a fundamental step preceding the translation of scientific findings to clinical application in humans. In most of these investigations, anesthetized animals are used to study cerebral function [14, 15, 16] The main reason for the use of anesthetics is that brain imaging requires immobilization of the subject inside the magnet, to generate meaningful and high signal-to-noise datasets. Immobilization, however, is a well-known stressor that induces important physiological changes that can severely influence the experimental results [17]. Therefore, animals are usually sedated/anesthetized before immobilization in the MRI setup [11, 12, 13, 14, 15, 17, 18]. As a side effect, however, anesthesia has an effect on the animal's physiology.

Mammals, such as laboratory mice, are endothermic animals, meaning that they are able to produce the heat necessary to regulate and maintain their body temperature (homeothermic) [19]. Temperature is therefore maintained within a stable range by physiological processes [20]. However, external agents, such as anesthetics, alter this physiological regulation in the animal [21] disrupting thermoregulation [22, 23, 24, 25, 26, 27]. The high body surface to weight ratio of the mouse makes it especially susceptible to hypothermia [28]. During anesthesia, body temperature decreases and must therefore be kept stable and within the physiological range in order to provide robust and quantitative fMRI signals. [29, 30, 31, 32, 33, 34].

fMRI data cannot be acquired without proper temperature control because the quantitative value of the measure would be lost. The reason is that vasodilation, and so the BOLD signal depends on body temperature [3]. Since most animal fMRI experiments are done under anesthesia, and since anesthesia affects temperature autoregulation [22], the animals must always be warmed to maintain a physiologic temperature. Therefore, what our development provides is an open-source, convenient and inexpensive way of controlling this vital parameter with high precision, instead of doing it manually.

For the reasons exposed above, a system to monitor and control the temperature of experimental animals is fundamental for fMRI experiments. Routinely, MRI setups are equipped with manual systems to control the temperature of the

experimental animals (most often mice and rats) monitoring the temperature with a MRI-compatible rectal probe and adjusting the temperature of a water bath connected to the bed of the animal or an air-heating system with a thermostat [35]. In this paper, an affordable Open-Source temperature control system for pre-crinical fMRI experimentation is presented. This automatic control device is designed for interconnecting and coordinating the necessary devices and actions for regulating temperature of an animal while being scanned. Employed accessories and components for communication between the different laboratory equipment and the Arduino microcontroller are presented. The experimental identification of the system thermal behavior is also studied and mathematically modeled. It verifies the design of the PID (proportional-integral-derivative) controller and the application of a control algorithm to regulate the temperature in anesthetized mice.

2. Materials and Methods

2.1. Overview

A temperature control system for anesthetized animals in preclinical scenarios has been developed. For this purpose, different subsystems were employed (Figure 1).

The core of the whole system is based on an Arduino MEGA 2560 (Smart Projects, Turin, Italy & SparkFun Electronics, Boulder, CO USA) with different "*shields*" attached. These "shields" are modules or boards that can be plugged on top of the Arduino PCB (Printed Circuit Board) for compact assembly. Currently, many platforms allow the users to develop their own microelectronic devices, with the Arduino (Smart Projects, Turin, Italy & SparkFun Electronics, Boulder, CO, USA) platform being one of the most renowned [36]. It is an open source hardware and software development platform whose basic principle is to facilitate a simple use of the hardware and software prototypes offer. Arduino has generated a large international community of users or makers (students, artists, programmers and professionals) who share their projects [37, 38, 39].

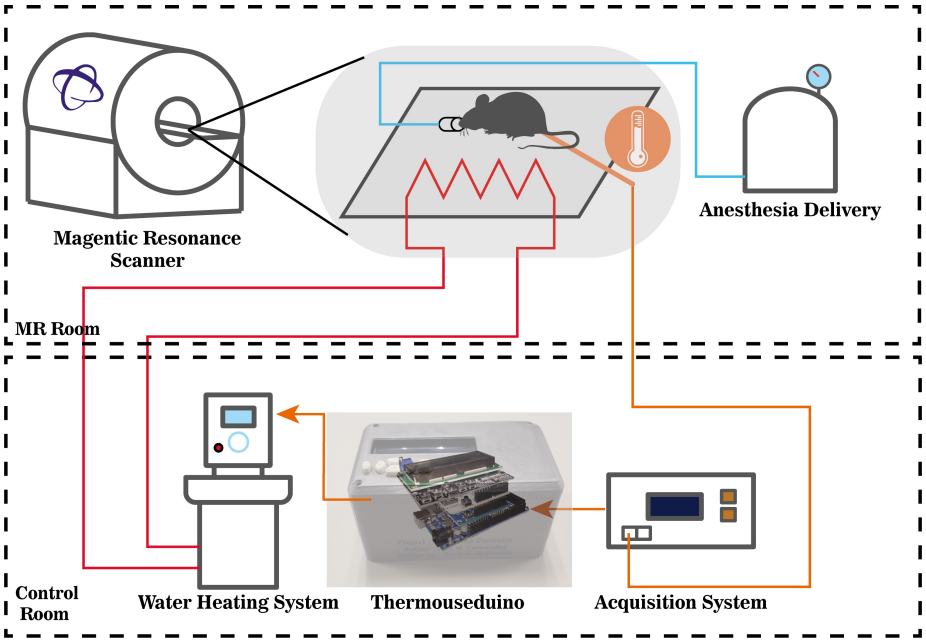

Figure 1: Schematic diagram of the connected devices. In the MRI room (upper part), the anesthetized animal is fixed to the MRI-bed, lying of a thermal water-pad connected to the water heating system (located in the Operator room). The optic-fiber temperature sensor is introduced into the rectum of the animal and connected to the OpSens Multisens signal conditioner and acquisition system in the Operator room. The TherMouseDuino interconnects the temperature acquisition system with the water heating device.

To warm up the anesthetized animal, a heated bath was employed. This bath allows control of the temperature of the fluid that warms the bed where the animal lies. An optical fiber sensor was used to measure body temperature due to its compatibility with the electromagnetic fields produced by the MR scanner. To set up the signal of the sensor, a signal conditioner with a serial communication port was employed.

2.2. Heating System

Thermo Scientific STANDARD Series Thermostats SC150 (ThermoFisher Scientific, Waltham, Massachusetts, USA) were attached to a Thermo Scientific SAHARA Heated Bath Circulator S5P (ThermoFisher Scientific, Waltham,

MA, USA) water bath, which pumps water through pipes to warm up the bed of the animal. Underneath this bed there is a pad, which is in direct contact with the animal. By modifying the reference temperature, it is possible to vary the temperature of the animal; however, these variations are neither linear nor immediate. Between the bath and the pad several thermal losses occur, due to the length of the tubing connecting them. This causes the temperature of the pad to not be exactly equal to that of the bath, but a few degrees below it. The bath consists of a thermal system that has its own time constant (a small reservoir in charge of storing the fluid and maintaining its temperature). The distance that the fluid must travel until it reaches the bed creates a delay between changes in the control action and the response of the actuator (the bath). In addition, the thermostat model has a protection system for high temperatures. This function is useful to prevent the animal from being burnt. Furthermore, it serves to protect the fluid conducting elements, which are not designed to conduct a fluid at very high temperatures. It also has a low-level liquid protection system, which stops pumping water when the liquid is below a threshold.

2.3. Acquisition Device

To obtain the body temperature of the animal an OTP-M Fiber Optic [40] high accuracy optical temperature sensor (Opsens Inc., Quebec, QC, Canada) is used together with the signal conditioner OpSens MultiSens signal conditioner (Opsens Inc., Quebec, QC, Canada). It consists of a sensor designed for medical applications approved by the FDA that offers high precision and resolution in temperatures measurement. The temperature sensor uses a glass specifically designed for this type of applications. The fiber optic transducer contains a temperature-sensitive optical device. In this case, since it is not a distributed temperature sensor, the temperature-sensitive zone is located at the tip of the sensor. The other end of the sensor is connected to the signal conditioner. This device is responsible for generating the light that passes through the optical fiber and, at the same time, for processing the received modified light signal, in order to convert these physical changes into units of measured temperature. The OTP-

M measures changes in the birefringence of the crystal used by the sensor. For this reason, there are no moving parts that could cause progressive deterioration of the sensor. These types of sensors are characterized by their high precision. Once the sensor is connected, configured and calibrated in the MultiSens signal conditioner, it is possible to visualize the temperature it measures. On the backside, it has a RS-232 connector for serial communication. Through this connection, it is possible to communicate externally with the MultiSens.

2.4. Microcontroller

The Arduino Mega 2560 development board is a printed circuit allowing the use of a microcontroller ATMEGA2560 (Figure 2A)[41]. Arduino is commonly used in a high variety of research fields due to its versatility and low cost [38, 42, 43, 44]. This microcontroller controls 54 digital Input/Output pins, 15 pulse width modulation pins, 16 analog pins and is able to automate any system. Documentation and software are open source and available at the Arduino website. The programming software is based on the C/C++ language. Programs can be adapted to the evolution of the project. The power supply of this development board can be done through USB or main supply from 5V to 12V.

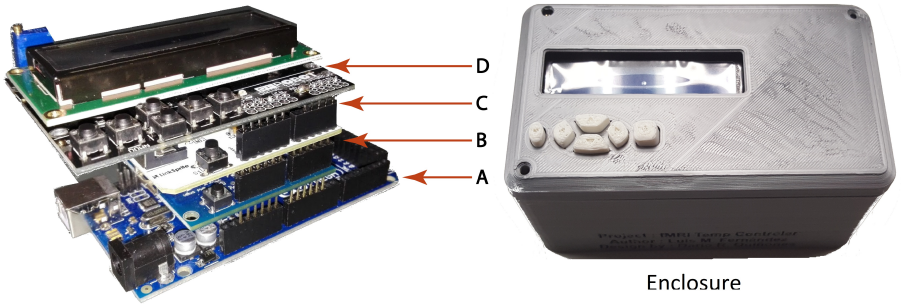

Figure 2: A) Arduino Mega 2560 development board. B) USB Host Shield V2.0 for USB communication with the ThermoScientific STANDARD Series Thermostat SC150. C) LinkSprite RS232 Shield V2 for RS-232 communication with the opSens Multisens signal conditioner. D) LCD Keypad Shield for the user interface.

2.5. Usb Host Module

For the communication of the Arduino with the thermostat SC150 the available USB port in the thermostat was used, meaning that, an additional USB port in the Arduino board was required. Using the USB Host Shield V2.0 for Arduino (Shenzhen KEYES DIY Robot co., Shen Zhen, China) (Figure 2B) it is possible to incorporate a standard type A USB port that allows communication with peripheral devices. This module incorporates the integrated MAX3421E, which includes the digital logic and analog circuitry required to implement a USB port according to the USB design specifications in version 2.0. This operation is controlled by accessing a series of registers through an SPI interface. In this way, the Arduino MEGA 2560 microprocessor can incorporate a USB port using the connections of the SPI interface. This allows several peripheral devices to be simultaneously connected to the microcontroller. Like the built-in module for RS-232 serial communication, the USB module allows direct connectivity with the Arduino, forming a compact multi-layer device.

2.6. RS-232 Communication Module

The above mentioned Arduino MEGA 2560 has only one USB port, used for communication with a personal computer and debugging, and a TTL UART interface. Nevertheless, to plug the signal acquisition device, a serial communication interface is needed. For this reason, an Arduino Shield with a RS-232 interface was attached to the Arduino Mega 2560. The LinkSprite RS232 Shield V2 (LinkSprite, Longmont, CO, USA) module for Arduino (Figure 2C) incorporates a DB9 port to the board. This module includes the integrated MAX232 and the necessary components to provide serial communication through the RS-232 standard. In addition, the RS232 Shield V2 design allows itself to be connected directly to Arduino, which improves their connection and permits a compact assembly.

2.7. LCD User Interface

To interact with the microcontroller, the LCD (Liquid Crystal Display) module Keypad Shield (DFrobot, Shanghai, China) for Arduino (Figure 2D) was

added. This shield incorporates an LCD and a five-button keyboard and acts as a user interface with the Arduino. This module provides a friendly user interface, permitting the user to move within the menus and to select the desired option. The screen consists of 2 rows and 16 columns. Furthermore, it also incorporates an additional microcontroller reset button. In the shield upper left corner, there is a potentiometer that allows the user to adjust the contrast of the LCD screen. This module provides the control of the temperature and it permits to display information (e.g. the selected reference temperature or the temperature of the animal).

2.8. Model Identification

Before designing the regulator, a mathematical approach to the system was obtained. The process of identifying a system model consists of finding mathematical equations that approach the behavior of the real system [45]. The model should be able to reproduce the outputs to different inputs. However, it should also be as simple as possible to achieve the objectives of the system quickly and without requiring a high computational demand. For this reason, it is necessary to reach a compromise between fidelity and computational cost. The system processes comprising the biological regulation mechanisms of the animal have a high degree of complexity, and they cannot be easily approximated using mathematical equations [46, 47]. For this reason, experimental identification was considered the most appropriate modeling method [45]. Unitary Step Response was the experimental methodology employed [48] for model identification. By means of this test, it is possible to determine the dynamic characteristics of the system and the output gain. The steps that are carried out for this type of identification are:

1. Move the system to the operating point. The first step was to bring the temperature of the system near the operating temperature.
2. When the temperature became steady, a positive step was entered as an input to the system [48]. In this case, the positive step was 2 °C.

3. When the new equilibrium was reached, the previous 2 °C increment was retracted to return to the initial operating point. As in the previous steps, it was necessary to wait for the system to regain equilibrium.
4. Finally, a negative step was introduced at system input with the same amplitude as the positive one, followed by repetition of steps 2 and 3.

After performing the mentioned steps, a system model was implemented in MATLAB (The Mathworks Inc., Natick, MA, USA). With the *System Identification Toolbox*, different models were obtained and, based on the percentage of adjustment, a model was chosen.

2.9. PID Control

A PID controller is a feedback control mechanism widely used in industrial control systems. This mechanism calculates the deviation or error between a measured value and a desired value. The PID control algorithm consists of three different parameters: proportional, integral and derivative. The proportional value depends on current error. The integral depends on past errors and the derivative is a prediction of future errors. The sum of these three actions is used to adjust the process by means of a control element such as the position of a control valve or the amount of power supplied to warm up a heater. For unknown processes, it has historically been considered that the PID controller is the most suitable controller. By adjusting these three variables in the PID control algorithm, the controller can provide a control action designed for specific process requirements. The controller response can be described in terms of a control response to an error, the degree to which the controller exceeds the desired setpoint (overshoot), and the degree of oscillation of the system. Some applications may only require one or two modes provided by this control system. PI controllers are particularly common because the derivative action is very sensitive to noise, and the absence of the integral process can prevent it from reaching the desired value due to the control action [49, 50].

2.10. Animals and MRI Acquisition Protocol

Some functional MRI experiments were carried out in order to test the effectivity of the TherMouseDuino in controlling mouse?s temperature and its impact over the evoked BOLD signal in real conditions. Experiments were carried out in a horizontal 7 T scanner with a 30 cm diameter bore (Biospec 70/30v, Bruker Medical, Ettlingen, Germany). The system has a 675 mT/m actively shielded gradient coil (Bruker, BGA 12-S) of 11.4 cm inner diameter. A 1H rat brain receive-only phase array coil with integrated combiner and preamplifier, no tune/no match, in combination with the actively detuned transmit-only resonator (BrukerBioSpin MRI GmbH, Germany) was employed. Data were acquired and processed with a Hewlett-Packard console running Paravision 5.1 software (Bruker Medical GmbH, Ettlingen, Germany) operating on a Linux platform. For the fMRI experiments, mice (n=3) were anesthetized with isoflurane (4% induction, 1-2% maintenance). Anesthetized animals were placed in a custom-made animal holder with adjustable bite and ear bars, and positioned on the magnet bed. The animals were constantly supplied with 0.8 L/m O2 with. The heart rate, SpO2, and breathing rate were monitored throughout the session (MouseOx, Starr Life Sciences, Oakmont, US). Temperature was controlled using the presented device.

2.11. Surgery for fMRI experiments

Mice were anaesthetized with urethane (1.4 g/kg) and fixed in a stereotaxic frame (Narishigue, Tokyo, Japan). We placed a custom made carbon fibre MRI-compatible electrode [16, 51] in the perforant pathway (-4.3 mm AP, -2.5 mm LM, +1.4 mm DV, 12 ° angle). Briefly, a bunch of 7 μm diameter carbon fibres (Goodfellow Cambridge Limited, Cambridge, UK) were introduced into a pulled double borosilicate capillary (WPI, ref. TST150-6") with $\cong$ 200m tip diameter and electrical impedance of 40-65 k Ω. A wire connector was couple to the carbon fibres using silver conductive epoxy resin (ref: 186-3616, RS components, Madrid, Spain) and isolated with rapid epoxy resin (Araldite, Basel, Switzerland). Pulled capillary tip was bent to form a 90 ° angle and

then implanted into the perforant pathway. The carbon fibre electrode was secured to the skull with super-bond C&B dental cement (Sun Medical Co. LTD, Moriyana, Shiga, Japan). Then the animals were carried to the fMRI facility and placed in a custom made animal holder with adjustable bite and ear bars and positioned into the horizontal 7-T scanner (Biospec 70/30, Bruker Medical, Ettlingen, Germany). Animals were constantly supplied with 0.8 L/min O2 through a mask. Temperature was set at 37 ° C using the developed device.

All experiments were approved by our institution's Animal Care and Use Committee and complies with the Spanish (law 53/2013) and European regulations (EU directive 86/609, EU decree 2001-486 and EU recommendation 2007/526/EC).

2.12. fMRI data extraction

Functional images acquisition was performed in coronal slices using a GE-EPI protocol applying the following parameters: field of view (FOV) 25x25 mm, slice thickness, 1 mm; matrix, 96x96; segments, 1; FA 60o; time echo (TE), 15 ms; time repetition (TR), 2000 ms. T2-weigthed anatomical images were collected using a rapid acquisition relaxation enhanced sequence (RARE): FOV, 25x25 mm; 12 slices; slice thickness, 1mm; matrix, 192x192; TEeff, 56 ms; TR, 2 s; RARE factor, 8. A 1H mouse brain received -only phased- array coil with integrated combiner and preamplifier, and no tune/no match, was employed in combination with the actively detuned transmit-only resonator (Bruker BioSpin MRI GmbH, Germany). Functional MRI data were analysed offline using our lab own software developed in MatLab, which included Statistical Parametric Mapping packages (SPM8, www.fil.ion.ucl.ac.uk/spm) and Analysis of Functional NeuroImages (AFNI, http://afni.nimh.nih.gov/afni). After linear detrending, temporal (0.015-0.2 Hz) and spatial filtering (3x3 gaussians kernel or 1.5 sigma) of voxel time series, a general linear model (GLM) was applied. Functional maps were generated from voxels that had a higher significance than $p < 0.01$.

3. Results and Discussion

3.1. Experimental Identification Results

Experimental identification of the model parameters was performed with a mouse in an fMRI experiment. First, the mouse was anesthetized and placed into the MR scanner. Due to the loss of thermoregulation induced by anesthesia, body temperature drops quickly below 33 °C (Figure 3). Initially, the water bath temperature was set at 45 °C. This temperature was selected to raise the body temperature of the mouse to the desired operating temperature (37 ± 0.5 °C). When the temperature of the animal had stabilized at 36.5 ± 0.3 °C, a positive step of 2 °C was applied, raising the bath temperature to 47 °C. This generated a variation in the body temperature of the animal, which is taken as output.

To study the abovementioned output as a response to the input (positive step), a data preprocessing was performed. It consisted of normalizing the data and selecting the necessary data window. (Figure 4). The output curve

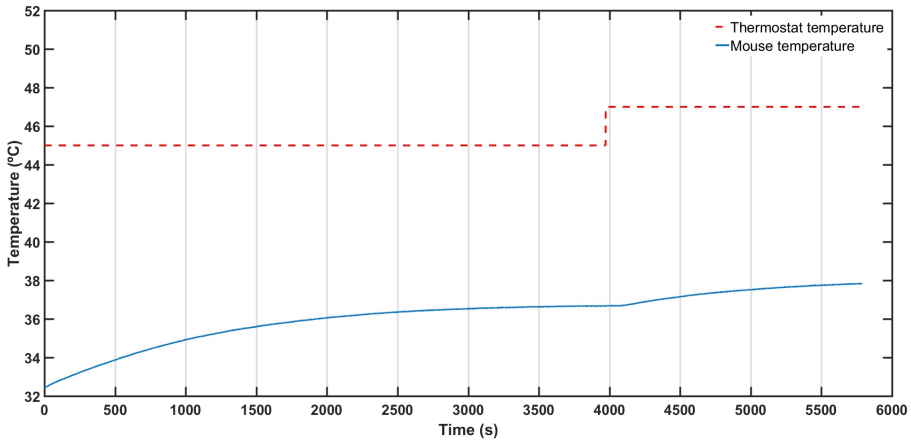

Figure 3: Data acquisition for experimental identification of the system. The data shown correspond to an fMRI experiment with a mouse. The dashed line shows a 2 °C positive step in the bath. The continuous line represents the body temperature of the mouse during the experiment. It is possible to observe that mouse body temperature starts to be stable at 3500 seconds (1 hour approximately) after the unitary step. The figure shows how the positive step in the heating system affects body temperature.

mimics the curve corresponding to a first-order system. However, there is a small delay between the input signal and the system response. This is due to a delay introduced by the dynamics of the actuators and the own physiology of the animal. When a new temperature is set in the bath thermostat, the fluid takes some time to reach that temperature.

Experimental identification must be a compromise between the complexity of the estimated model and the benefit that this complexity reports. A mathematical model was calculated from the above mentioned data as shown in Figure 5. This mathematical model has a small difference in the percentage of fit between a first-order model and greater order models. Therefore, the first-order model without delay ('TF (fit 91,49%)' in Figure 5) was selected. The estimated model for the mouse system is shown in Equation 1.

$$G(s) = \frac{K}{1 + \tau \cdot s} = \frac{0.6792}{1 + 952.38 \cdot s} \tag{1}$$

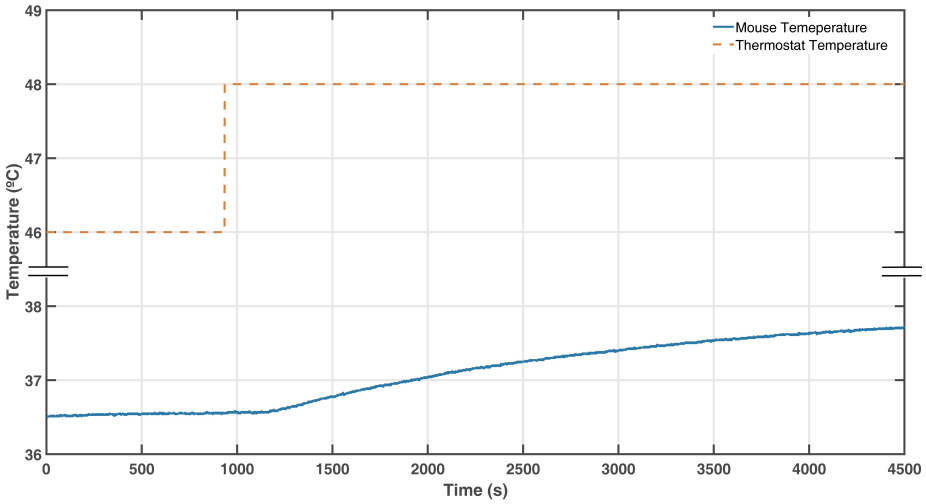

Figure 4: Selected data for the experimental identification of the system. This graph displays the response of body temperature of the animal against a 2 °C increase in the thermostat temperature. The selected and normalized data window was employed for the experimental identification. The dashed line shows the input temperature positive step applied to the system. The continuous line shows the body temperature of the mouse during the experiment

where the static gain of the system $K = 0.6792$ and the time constant $\tau = 952.38$ seconds ($\cong$ 16 minutes).

3.2. Control System Design Results

Once an approximate model of the real system was obtained, the next step was to translate the specifications that the control system must meet to mathematical constraints. With reference to dynamic specifications, one of the requested conditions was establishment time (t_e). This condition was adjusted to experiment preparation time, that is, 30 to 45 minutes used in the placement of the animal, survey images, and adjustments for the homogeneity of the magnetic field. The regulator was required to be able to reach the reference temperature within that time range. Next, it was desired that the temperature in steady state at a physiological level of $37 \pm 0.5\,^{\circ}$C. Additionally, an overshoot not exceeding $37.5\,^{\circ}$C was required, in keeping with physiological temperature. In terms of steady error, this should be zero. However, this condition will be extremely demanding for a thermal system. Due to this fact, the acceptable error was established at $\pm$ $0.5\,^{\circ}$C. Finally, an oscillation in steady state was deemed undesirable. To avoid overheating or burning the skin of the animal,

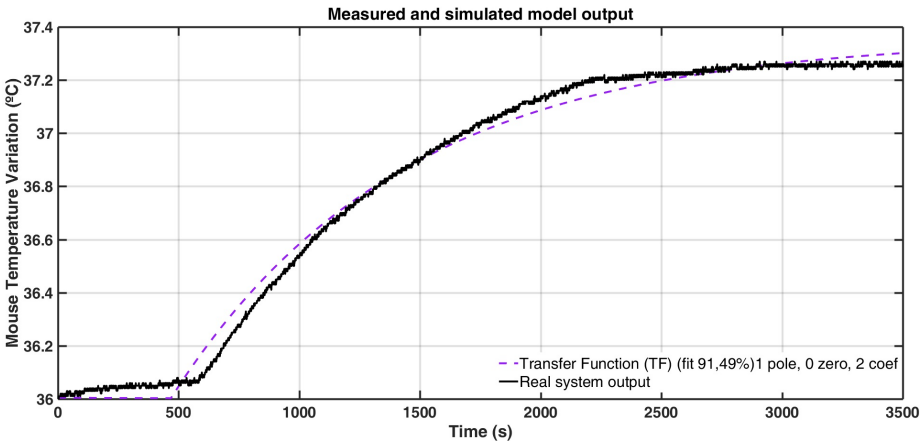

Figure 5: Measured and simulated model output. This image displays the output of the real system against a positive step input (continuous line) and, the simulated output of the final mathematical model (Transfer Function).

the control action was limited to 50 °C. High control actions will not represent the real control system because the abovementioned limit will not allow them. These constrains limit the design of the control system. These specifications were transferred to the MATLAB control systems design tool. Using the mentioned tool, the root locus of the system with all the constraints was calculated. This corresponds to a unit gain proportional controller (i.e. output is directly proportional to input). However, there is one main drawback, this system does not ensure a null error in the steady state. In order to solve this, an integral control action was introduced along with the proportional action to ensure the minimal stationary error. The PI regulator equation in zeros and poles form is shown in Equation 2.

$$PI(s) = \frac{K_R(s+b)}{s} \tag{2}$$

The tuning of the regulator consists of obtaining values of K_R and b that allow fulfillment of the specifications in closed loop. The PI regulator consists of a pole at the origin and a zero. The method used for tuning the regulator is the poles and zeros adjustment [45]. A zero is added to a tenth of the pole of the system ($b = 0.000105$). This zero was required to know the Integrative Time (Ti) as is shown in Equation 3

$$Ti = \frac{1}{b} \tag{3}$$

The goal is not to overturn the root locus. This zero adjustment is called "the empirical criterion". The last step is tuning the gain in order for the specifications to be achieved. We decided to select an energetic PI regulator with a K=5. This can cause saturation of the control action, but it is necessary to accelerate the process as much as possible in order to meet the establishment time specification. To eliminate the steady state error, the integral control action was increased. The steady state error was eliminated with an integer value of $Ki = 0.01$, but a small overshoot was introduced in the system response

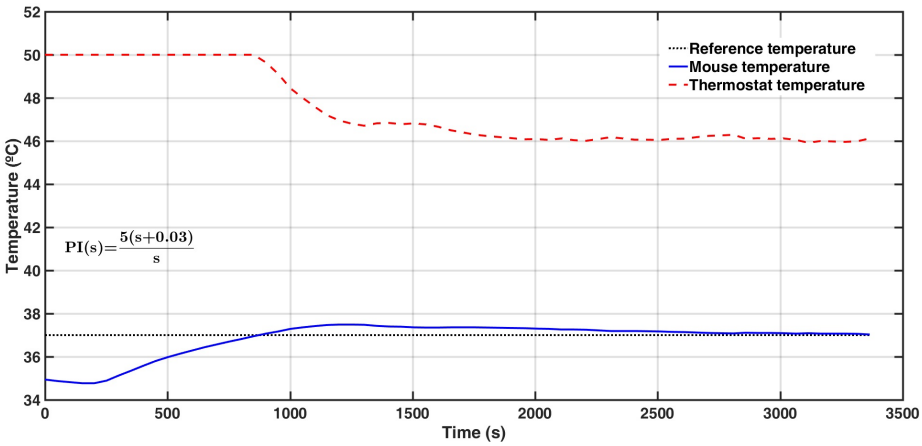

Figure 6: Results obtained using the final regulator. This figure shows the results for the final PI regulator meeting the required specifications. It shows the data output obtained in an fMRI experiment with an anesthetized mouse. The body temperature of the mouse (continuous line) and the thermostat temperature (dotted line) are shown.

(Equation 4).

$$Ki = \frac{K}{Ti} \tag{4}$$

Nevertheless, this overshoot was acceptable with the required specifications, since it did not exceed the temperature of 37.5 °C. The set-up time is around 2700 seconds (45 minutes), which is in conformity with the specifications. Finally, the accepted parameters for the PI controller and the results obtained are shown in Figure 6. An overshoot still appears at the system output, but we deem it to be within the acceptable range. This corresponds to one of the required specifications. In addition, the temperature oscillations around the reference were negligible.

The regulator is responsible for maintaining this temperature with the smallest possible error. This allows reduction of the setup time necessary for image acquisition and provides automatically a stable temperature through the course of the fMRI experiment.

An example of fMRI experiment in mice can be seen in Figure 7A and Figure 7B. In this study we stimulate the perforant pathway, main input from

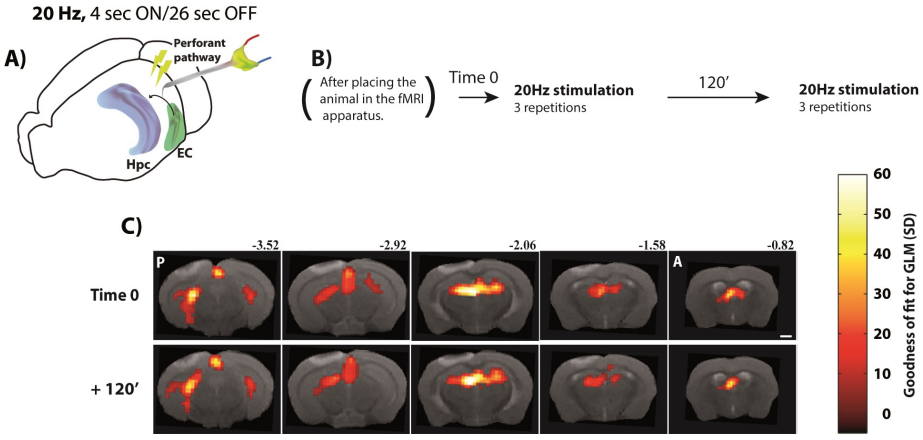

Figure 7: BOLD response for 20Hz electric stimulation in the perforant pathway. A) Scheme of the carbon fibre electrode implanted in the performant pathway. B) Timing of the fMRI acquisitions in the experiment. C) Representative T2-weighted anatomy images with overlaid functional maps evoked during stimulation of the perforant pathway (20Hz, 0.8 mA). Scale indicates 1 mm. Colour-bar indicates the goodness of fit for the General Linear Model (GLM) applied, comparing activation during the 20 Hz stimulation train (ON period, 4 sec) vs. baseline (OFF period, 26 sec). Numbers above the images represent mm from bregma. P: posterior; A: anterior. Threshold for GLM significance set on $p < 0.01$.

the entorhinal cortex to the hippocampus, to investigate the global consequences of local synaptic plasticity (i.e. [51, 52]).

These experiments require long periods of brain imaging to monitor longitudinally the consequences of short- and long-term plasticity. During the complete recording time, the physiology of the animal needs to be exquisitely constant, in order to preserve the quantitative value of the BOLD signals [11, 16, 35]. Only a control experiment without induction of synaptic plasticity is shown in Figure 7C, to illustrate the high stability of the signal in time.

4. Conclusions

Results obtained by fMRI based on the BOLD contrast are very sensitive to physiological changes. The use of anesthetics for experimentation with animals causes alterations in their temperature regulation system. This translates into

important variations in the MRI images obtained. Commonly used systems to maintain body temperature are manual, requiring continuous inspection by the researcher or the technician performing the experiment. By using an automatic control system based on Arduino we have developed an Open-Source temperature control device for fMRI experimentation in mice. Model and experimental result demonstrate the viability of the system for maintaining the temperature of the anesthetized animal within the physiological range and meeting user specifications that assure its practical use. TherMouseDuino can control both, increases and decreases in temp. It just need to be coupled to the specific hardware (e.g. a cooler system). TherMouseDuino therefore, provides an automatic, safe and precise control of body temperature for anesthetized mice. It was tested with strain C57 (inbred line) and ICR (outbred line) with the same satisfactory result in both cases. In addition, all the schematics, parts and firmware are available at http://dmoratal.webs.upv.es/research.html.

Funding

This work was supported in part by the Spanish Ministerio de Economía y Competitividad (MINECO) and FEDER funds under grants BFU2015-64380-C2-2-R (D.M.) and BFU2015-64380-C2-1-R and EU Horizon 2020 Program 668863-SyBil-AA grant (S.C.). S.C. acknowledges financial support from the Spanish State Research Agency, through the "Severo Ochoa" Programme for Centres of Excellence in R&D (ref. SEV- 2013-0317). D.R.Q. was supported by grant "Ayudas para la formación de personal investigador (FPI)" from the Vicerrectorado de Investigación, Innovación y Transferencia of the Universitat Politècnica de València.

Acknowledgements

The authors are also grateful to Begoña Fernández for their technical support.

References

[1] N. K. Logothetis, The neural basis of the blood-oxygen-level-dependent functional magnetic resonance imaging signal, Philosophical Transactions of the Royal Society B: Biological Sciences 357 (1424) (2002) 1003–1037. doi:10.1098/rstb.2002.1114.

[2] B. B. Biswal, J. Van Kylen, J. S. Hyde, Simultaneous assessment of flow and BOLD signals in resting-state functional connectivity maps., NMR in biomedicine 10 (4-5) (1997) 165–70.

[3] J. L. Boxerman, L. M. Hamberg, B. R. Rosen, R. M. Weisskoff, MR contrast due to intravascular magnetic susceptibility perturbations, Magnetic Resonance in Medicine 34 (4) (1995) 555–566. doi:10.1002/mrm.1910340412.

[4] H. Gudbjartsson, S. Patz, Simultaneous calculation of flow and diffusion sensitivity in steady-state free precession imaging, Magnetic Resonance in Medicine 34 (4) (1995) 567–579. doi:10.1002/mrm.1910340413.

[5] I. Digernes, A. Bjørnerud, S. A. S. Vatnehol, G. Løvland, F. Courivaud, E. Vik-Mo, T. R. Meling, K. E. Emblem, A theoretical framework for determining cerebral vascular function and heterogeneity from dynamic susceptibility contrast MRI, Journal of Cerebral Blood Flow & Metabolism 37 (6) (2017) 2237–2248. doi:10.1177/0271678X17694187.

[6] K. Johar, A. Priya, M. T. T. Wong-Riley, Regulation of Na + /K + -ATPase by nuclear respiratory factor 1, Journal of Biological Chemistry 287 (48) (2012) 40381–40390. doi:10.1074/jbc.M112.414573.

[7] C. Reynell, J. J. Harris, The BOLD signal and neurovascular coupling in autism, Developmental Cognitive Neuroscience 6 (2013) 72–79. doi:10.1016/j.dcn.2013.07.003.

[8] J. C. Whitman, L. M. Ward, T. S. Woodward, Patterns of cortical oscillations irganize neural activity into whole-brain functional networks Evident

in the fMRI BOLD signal, Frontiers in Human Neuroscience 7 (2013) 80. doi:10.3389/fnhum.2013.00080.

[9] C. J. Keller, S. Bickel, C. J. Honey, D. M. Groppe, L. Entz, R. C. Craddock, F. A. Lado, C. Kelly, M. Milham, A. D. Mehta, Neurophysiological investigation of spontaneous correlated and anticorrelated fluctuations of the BOLD Signal, Journal of Neuroscience 33 (15) (2013) 6333–6342. doi:10.1523/JNEUROSCI.4837-12.2013.

[10] K. R. Thulborn, D. Davis, P. Erb, M. Strojwas, J. A. Sweeney, Clinical fMRI: Implementation and Experience, NeuroImage 4 (3) (1996) S101–S107. doi:10.1006/nimg.1996.0060.

[11] A. Moreno, P. Jego, F. de la Cruz, S. Canals, Neurophysiological, metabolic and cellular compartments that drive neurovascular coupling and neuroimaging signals, Frontiers in Neuroenergetics 5 (2013) 3. doi:10.3389/fnene.2013.00003.

[12] S. Canals, M. Beyerlein, H. Merkle, N. K. Logothetis, Functional MRI Evidence for LTP-Induced Neural Network Reorganization, Current Biology 19 (5) (2009) 398–403. doi:10.1016/j.cub.2009.01.037.

[13] N. K. Logothetis, J. Pauls, M. Augath, T. Trinath, A. Oeltermann, Neurophysiological investigation of the basis of the fMRI signal, Nature 412 (6843) (2001) 150–157. doi:10.1038/35084005.

[14] J. Paasonen, R. A. Salo, A. Shatillo, M. M. Forsberg, J. Närväinen, J. K. Huttunen, O. Gröhn, Comparison of seven different anesthesia protocols for nicotine pharmacologic magnetic resonance imaging in rat., European neuropsychopharmacology : the journal of the European College of Neuropsychopharmacology 26 (3) (2016) 518–31. doi:10.1016/j.euroneuro.2015.12.034.

[15] K. A. Williams, M. Magnuson, W. Majeed, S. M. LaConte, S. J. Peltier, X. Hu, S. D. Keilholz, Comparison of α-chloralose, medetomidine and

isoflurane anesthesia for functional connectivity mapping in the rat, Magnetic Resonance Imaging 28 (7) (2010) 995–1003. doi:10.1016/j.mri.2010.03.007.

[16] L. Pérez-Cervera, J. M. Caramés, L. M. Fernández-Mollá, A. Moreno, B. Fernández, E. Pérez-Montoyo, D. Moratal, S. Canals, J. Pacheco-Torres, Mapping Functional Connectivity in the Rodent Brain Using Electric-Stimulation fMRI., Methods in molecular biology (Clifton, N.J.) 1718 (2018) 117–134. doi:10.1007/978-1-4939-7531-0_8.

[17] H. Senoo, Physiology of Stress and Starvation-like Conditions, in: The Laboratory Rat, Elsevier, 2000, pp. 447–460. doi:10.1016/B978-012426400-7.50062-5.

[18] S. Wegener, E. C. Wong, Longitudinal MRI studies in the isoflurane-anesthetized rat: long-term effects of a short hypoxic episode on regulation of cerebral blood flow as assessed by pulsed arterial spin labelling, NMR in Biomedicine 21 (7) (2008) 696–703. doi:10.1002/nbm.1243.

[19] N. C. Owens, Y. Ootsuka, K. Kanosue, R. M. McAllen, Thermoregulatory Control of Sympathetic Fibres Supplying the Rat's Tail, The Journal of Physiology 543 (3) (2002) 849–858. doi:10.1113/jphysiol.2002.023770.

[20] P. E. Sharp, M. C. LaRegina, The laboratory rat, Academic Press, 1998.

[21] C. Huang, O. T.-W. Ng, Y.-S. Ho, M. G. Irwin, R. C.-C. Chang, G. T.-C. Wong, Effect of Continuous Propofol Infusion in Rat on Tau Phosphorylation with or without Temperature Control, Journal of Alzheimer's Disease 51 (1) (2016) 213–226. doi:10.3233/JAD-150645.

[22] M. K. Huss, H. H. Chum, A. G. Chang, K. Jampachairsi, C. Pacharinsak, The Physiologic Effects of Isoflurane, Sevoflurane, and Hypothermia Used for Anesthesia in Neonatal Rats (Rattus norvegicus)., Journal of the American Association for Laboratory Animal Science : JAALAS 55 (1) (2016) 83–8.

[23] A. Schroeter, F. Schlegel, A. Seuwen, J. Grandjean, M. Rudin, Specificity of stimulus-evoked fMRI responses in the mouse: The influence of systemic physiological changes associated with innocuous stimulation under four different anesthetics, NeuroImage 94 (2014) 372–384. doi:10.1016/j.neuroimage.2014.01.046.

[24] E. Jonckers, R. Delgado y Palacios, D. Shah, C. Guglielmetti, M. Verhoye, A. Van der Linden, Different anesthesia regimes modulate the functional connectivity outcome in mice, Magnetic Resonance in Medicine 72 (4) (2014) 1103–1112. doi:10.1002/mrm.24990.

[25] T. Wu, J. Grandjean, S. C. Bosshard, M. Rudin, D. Reutens, T. Jiang, Altered regional connectivity reflecting effects of different anesthesia protocols in the mouse brain, NeuroImage 149 (2017) 190–199. doi:10.1016/j.neuroimage.2017.01.074.

[26] F. Schlegel, A. Schroeter, M. Rudin, The hemodynamic response to somatosensory stimulation in mice depends on the anesthetic used: Implications on analysis of mouse fMRI data, NeuroImage 116 (2015) 40–49. doi:10.1016/j.neuroimage.2015.05.013.

[27] J. Grandjean, A. Schroeter, I. Batata, M. Rudin, Optimization of anesthesia protocol for resting-state fMRI in mice based on differential effects of anesthetics on functional connectivity patterns, NeuroImage 102 (2014) 838–847. doi:10.1016/j.neuroimage.2014.08.043.

[28] P. Flecknell, Laboratory animal anesthesia: A practical introduction for research workers and technicians., Academic Press Inc., San Diego, 1996.

[29] G. Dispersyn, L. Pain, Y. Touitou, Circadian disruption of body core temperature and rest-activity rhythms after general (Propofol) Anesthesia in Rats, Anesthesiology 110 (6) (2009) 1305–1315. doi:10.1097/ALN.0b013e3181a10225.

[30] E. A. Kiyatkin, The hidden side of drug action: brain temperature changes induced by neuroactive drugs, Psychopharmacology 225 (4) (2013) 765–780. doi:10.1007/s00213-012-2957-9.

[31] M. S. Smirnov, E. A. Kiyatkin, Behavioral and temperature effects of delta 9-tetrahydrocannabinol in human-relevant doses in rats, Brain Research 1228 (2008) 145–160. doi:10.1016/j.brainres.2008.06.069.

[32] E. Kiyatkin, P. Brown, Brain and body temperature homeostasis during sodium pentobarbital anesthesia with and without body warming in rats, Physiology & Behavior 84 (4) (2005) 563–570. doi:10.1016/j.physbeh.2005.02.002.

[33] T. Tsurugizawa, Y. Takahashi, F. Kato, Distinct effects of isoflurane on basal BOLD signals in tissue/vascular microstructures in rats, Scientific Reports 6 (1) (2016) 38977. doi:10.1038/srep38977.

[34] N. P. Blockley, V. E. M. Griffeth, A. B. Simon, R. B. Buxton, A review of calibrated blood oxygenation level-dependent (BOLD) methods for the measurement of task-induced changes in brain oxygen metabolism, NMR in Biomedicine 26 (8) (2013) 987–1003. doi:10.1002/nbm.2847.

[35] J. Pacheco-Torres, A. Moreno, B. Fernández, L. Pérez-Cervera, J. Caramés, L. Fernández-Mollá, E. Pérez-Montoyo, D. Moratal, S. Canals, Functional MRI of synaptic plasticity, in "Handbook of in vivo neural plasticity techniques: A systems neuroscience approach to the neural basis of memory and cognition", Elsevier, Amsterdam, The Netherlands, 2018.

[36] J. Guerreiro, A. Lourenço, H. Silva, A. Fred, Performance Comparison of Low-cost Hardware Platforms Targeting Physiological Computing Applications, Procedia Technology 17 (2014) 399–406. doi:10.1016/j.protcy.2014.10.204.

[37] G. Lockridge, B. Dzwonkowski, R. Nelson, S. Powers, Development of a

Low-Cost Arduino-Based Sonde for Coastal Applications, Sensors 16 (4) (2016) 528. doi:10.3390/s16040528.

[38] P. Teikari, R. P. Najjar, H. Malkki, K. Knoblauch, D. Dumortier, C. Gronfier, H. M. Cooper, An inexpensive Arduino-based LED stimulator system for vision research., Journal of neuroscience methods 211 (2) (2012) 227–36. doi:10.1016/j.jneumeth.2012.09.012.

[39] P. Artoni, S. Landi, S. S. Sato, S. Luin, G. M. Ratto, Arduino Due based tool to facilitate in vivo two-photon excitation microscopy, Biomedical Optics Express 7 (4) (2016) 1604. doi:10.1364/BOE.7.001604.

[40] V. A. Korolyov, V. T. Potapov, Biomedical fiber-optic temperature and pressure sensors, Biomedical Engineering 46 (2) (2012) 79–82. doi:10.1007/s10527-012-9272-y.

[41] A. D'Ausilio, Arduino: a low-cost multipurpose lab equipment., Behavior research methods 44 (2) (2012) 305–13. doi:10.3758/s13428-011-0163-z.

[42] T. Besson, D. Debayle, S. Diochot, M. Salinas, E. Lingueglia, Low cost venom extractor based on Arduino board for electrical venom extraction from arthropods and other small animals, Toxicon 118 (2016) 156–161. doi:10.1016/j.toxicon.2016.05.001.

[43] A. Sheinin, A. Lavi, I. Michaelevski, StimDuino: An Arduino-based electrophysiological stimulus isolator, Journal of Neuroscience Methods 243 (2015) 8–17. doi:10.1016/j.jneumeth.2015.01.016.

[44] A. S. Ali, Z. Zanzinger, D. Debose, B. Stephens, Open Source Building Science Sensors (OSBSS): A low-cost Arduino-based platform for long-term indoor environmental data collection, Building and Environment 100 (2016) 114–126. doi:10.1016/j.buildenv.2016.02.010.

[45] K. Ogata, Y. Yang, Modern control engineering, 5th Edition, Pearson Education, Upper Saddel River, New Jersey, 1990.

[46] A. Shitzer, E. Arens, H. Zhang, Compilation of basal metabolic and blood perfusion rates in various multi-compartment, whole-body thermoregulation models, International Journal of Biometeorology 60 (7) (2016) 1051–1064. doi:10.1007/s00484-015-1096-5.

[47] J. M. Barker, C. E. Cooper, P. C. Withers, A. P. Cruz-Neto, Thermoregulation by an Australian murine rodent, the ash-grey mouse (Pseudomys albocinereus), Comparative Biochemistry and Physiology Part A: Molecular & Integrative Physiology 163 (3-4) (2012) 336–342. doi:10.1016/j.cbpa.2012.07.011.

[48] R. C. Dorf, N. K. Sinha, Modern Control Systems, IEEE Transactions on Systems, Man, and Cybernetics 11 (8) (1981) 580–580. doi:10.1109/TSMC.1981.4308749.

[49] I. J. Koenka, J. Sáiz, P. C. Hauser, Instrumentino: an open-source software for scientific instruments, CHIMIA International Journal for Chemistry 69 (4) (2015) 172–175.

[50] R. Anderson, D. Cervo, Pro Arduino, in: Pro Arduino, Vol. 28, Apress, Berkeley, CA, 2013, Ch. 7, p. 316. doi:10.1007/978-1-4302-3940-6.

[51] A. Moreno, R. G. Morris, S. Canals, Frequency-Dependent Gating of HippocampalNeocortical Interactions, Cerebral Cortex 26 (5) (2016) 2105–2114. doi:10.1093/cercor/bhv033.

[52] E. Alvarez-Salvado, V. Pallares, A. Moreno, S. Canals, Functional MRI of long-term potentiation: imaging network plasticity, Philosophical Transactions of the Royal Society B: Biological Sciences 369 (1633) (2013) 20130152–20130152. doi:10.1098/rstb.2013.0152.